First-principles study of thin magnetic transition-metal silicide films on Si(001)

Hua Wu, Peter Kratzer, and Matthias Scheffler

Fritz-Haber-Institut der Max-Planck-Gesellschaft, Faradayweg 4-6, D-14195 Berlin, Germany

In order to combine silicon technology with the functionality of magnetic systems, a number of ferromagnetic (FM) materials have been suggested for the fabrication of metal/semiconductor heterojunctions. In this work, we present a systematic study of several candidate materials in contact with the Si surface. We employ density-functional theory calculations to address the thermodynamic stability and magnetism of both pseudomorphic CsCl-like MSi (M=Mn, Fe, Co, Ni) thin films and Heusler alloy M_2MnSi (M=Fe, Co, Ni) films on Si(001). Our calculations show that Si-termination of the MSi films is energetically preferable during epitaxy since it minimizes the energetic cost of broken bonds at the surface. Moreover, we can explain the calculated trends in thermodynamic stability of the MSi thin films in terms of the M-Si bond-strength and the M $3d$ orbital occupation. From our calculations, we predict that ultrathin MnSi films are FM with sizable spin magnetic moments at the Mn atoms, while FeSi and NiSi films are nonmagnetic. However, CoSi films display itinerant ferromagnetism. For the M_2MnSi films with Heusler-type structure, the MnSi termination is found to have the highest thermodynamic stability. In the FM ground state, the calculated strength of the effective coupling between the magnetic moments of Mn atoms within the same layer approximately scales with the measured Curie temperatures of the bulk M_2MnSi compounds. In particular, the Co$_2$MnSi/Si(001) thin film has a robust FM ground state as in the bulk, and is found to be stable against a phase separation into CoSi/Si(001) and MnSi/Si(001) films. Hence this material is of possible use in FM-Si heterojunctions and deserves further experimental investigations.

PACS numbers: 75.70.-i, 73.20.At, 68.35.Md

I. INTRODUCTION

Metal-semiconductor heterojunctions have received much attention in the context of magnetoelectronics or spintronics because they could open up the possibility to inject a spin-polarized current from a ferromagnetic (FM) metal into a semiconductor. This is a pre-requisite for anticipated future electronic devices making use of spin-polarized carriers.[1] In this paper, we present theoretical investigations of thin films for two materials classes relevant in this context, namely transition metal (TM) mono-silicides, MSi (M= Mn, Fe, Co, Ni), in the CsCl crystal structure, and Heusler alloys M_2MnSi (M= Fe, Co, Ni). The two materials classes are closely related in their crystal structure. Pictorially, one can think of M_2MnSi films as being formed by the substitution of Mn for half of the Si atoms in each Si layer of the CsCl-like MSi (M=Fe, Co, Ni) films. Both materials classes are of potential interest for spintronics applications. Some Heusler alloys, like Co$_2$MnZ (Z=Si, Ge, Sn) are ferromagnets even well above room temperature, and are predicted by band theory to be magnetic half-metals, i.e., the Fermi energy lies in a region of partially occupied bands for one spin channel, while lying in a gap of the density of states in the other.[2,3,4] Therefore half-metallic Heusler alloys can in principle provide 100% spin-polarized carriers, and could thus serve as spin-filters in future spintronics devices. However, also the structurally simpler mono-silicides have a potential to be applied in spintronics devices: Recently, we have shown that thin MnSi films on Si(001) possess sizable magnetic moments at the Mn atoms,[5] despite the fact that bulk MnSi (in the corresponding hypothetical CsCl crystal structure) is nonmagnetic. Moreover, calculations of CoSi in CsCl crys-

tal structure find this (metastable) compound to be ferromagnetic. This motivated us to study systematically both the structural and magnetic properties of late TM mono-silicides films. In addition, mixed TM silicides have also attracted interest, since evidence has been given that FeSi could be made ferromagnetic by doping with Co.[6,7]

From the viewpoint of applications, it is highly desirable to grow well-defined FM metallic films on the most common semiconductor, silicon, in particular on the technologically relevant Si(001) surface. For this reason, we concentrate in the present paper on pseudomorphic thin films of mono-silicides and Heusler alloys on Si(001). For epitaxial growth, the mono-silicides in CsCl-like crystal structure are particularly attractive: We find that the CsCl structure is a metastable phase of the mono-silicides, only moderately higher in energy than the ground state crystal structure, and it is closely lattice-matched with Si(001). Moreover, such CoSi and NiSi crystals have been found to be 'supersoft' materials,[8] i.e., there is a range of elastic deformations with very little energetic cost. The Heusler alloys show a somewhat larger lattice-mismatch with Si(001) of about 4%. Apart from good lattice-match, flat and atomically sharp interfaces are of crucial importance for efficient spin injection. In this context, it is noteworthy that di-silicide films have been grown with atomically sharp interfaces to Si(111) and Si(100). The CaF$_2$ crystal structure of di-silicides is similar to the CsCl crystal structure of mono-silicides (it results if each second metal site in the CsCl structure is left vacant). This suggests that film growth with atomically sharp interface should also be possible for the mono-silicides films. In practice, first a buffer layer of the di-silicide is grown, followed by growth of the mono-silicide film. With this strategy, CsCl-like FeSi and CoSi

films have already been grown on Si(111) by von Känel et al.[9,10]

While theoretical investigations of CsCl-like MSi thin films on Si(001) are scarce,[11] a group of studies addressing the initial reaction processes of TM adatoms with the Si substrate report that Mn, Co and Ni adatoms prefer subsurface sites.[5,12,13,14] Heusler alloy films have been studied experimentally mostly in view of their application in tunnelling magneto-resistance devices.[15,16,17] Concerning epitaxial growth on semiconductor substrates, results for thin Co_2MnGe[18] and Co_2MnSi[19] films on GaAs(001) have been reported. From the theoretical side, calculations of the $Co_2MnSi(001)$ surface,[20,21] as well as of the interface between Co_2MnGe and GaAs(001)[22,23] have been performed.

In the present paper, we identify the trends in chemical bonding, thermodynamic stability, and magnetism of the MSi and M_2MnSi thin films. Most importantly, our calculations predict that, in addition to ultrathin FM MnSi/Si(001) films,[5] the CoSi/Si(001) thin films are also FM; and that Co_2MnSi/Si(001) films have a robust FM ground state.

II. COMPUTATIONAL DETAILS

The present DFT calculations were performed using the all-electron full-potential augmented plane-wave plus local-orbital method.[24] The generalized gradient approximation (GGA)[25] was adopted for the exchange-correlation potential, since it has been shown[26,27] that GGA gives a better description for both transition metals and their silicides than the local-spin-density approximation. The MSi or M_2MnSi thin films on Si(001) were modelled by a slab consisting of eight successive Si(001) layers and the MSi (see Fig. 1) or M_2MnSi layers (see Section III C) on both sides, in order to retain the inversion symmetry. The GGA calculated equilibrium lattice constant (5.48 Å) of bulk Si is used for the Si(001) substrate. A supercell with about 10-11 Å vacuum between the slabs, and with a lateral (1×1) periodicity[5] (lattice constant of 3.87 Å) was used. Note that θ=1 ML (monolayer) coverage of M refers to two M adatoms per (1×1) cell on either side of the slab. The muffin-tin radii are chosen to be 1.11 Å for Mn, as used in our previous calculations,[5] and 1.06 Å for Fe, Co, Ni, and Si, in order to avoid overlap of the muffin-tin spheres (due to covalent bond-shortening within the TM silicide series, as we report below) during structure relaxations. This choice is reasonable in view of their respective atomic sizes. The cut-off energy for the interstitial plane-wave expansion is chosen to be 15.2 Ryd.[28] A set of $10 \times 10 \times 1$ special $\mathbf{k}$ points is used for integrations over the Brillouin zone of the (1×1) surface cell. Except for the two central Si layers in the slab, all the M and other Si atoms are relaxed until the calculated atomic force for each of them is smaller than 0.05 eV/Å. Throughout this paper,
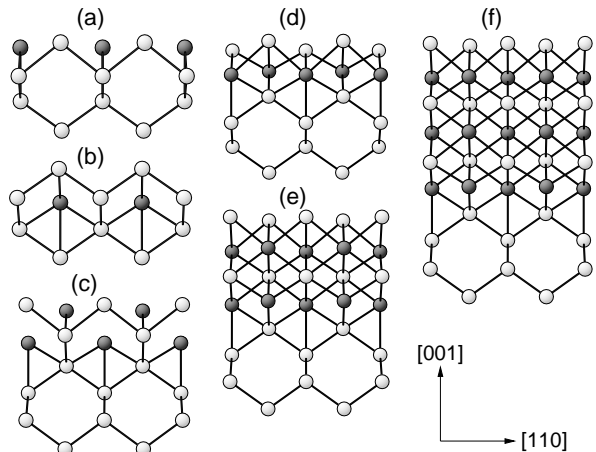

FIG. 1: Side view of various M=Mn, Fe, Co, or Ni films on Si(001) (half of the slab), with 0.5 ML M in (a) the first- or (b) second-layer interstitial sites, 1 ML M (c) in a mixed layer or (d) in a Si-M sandwich, or (e) 2 ML or (f) 3 ML M CsCl-like sandwich structures. Black balls represent M and gray balls Si atoms. The bonds shorter than 2.65 Å are shown.

formation energies are given per (1×1) cell, defined as

$$E_{\text{form}} = (E_{\text{tot}} - \sum_i N_i \mu_i)/2 - \gamma_{\text{Si}} A, \qquad (1)$$

where E_{tot}, N_i and μ_i refer to the total energy per (1×1) unit cell with surface area A, the number of atoms of each chemical type in the cell, and their chemical potentials as calculated from the corresponding bulk materials. The factor 2 in the denominator is because the slab contains two equivalent surfaces due to the inversion symmetry. γ_{Si}=84 meV/Å^2 is the surface energy of the clean, $p(2 \times 2)$-reconstructed Si(001) surface. We note that E_{form} defined in this way contains the bulk heat of formation, as well as surface and interface contributions. The interface energy alone, which could serve as an indicator for adhesion of the films to the substrate, is not considered. The numerical accuracy of the present calculations is carefully checked by using higher cut-off energy and more $\mathbf{k}$ points. With these settings, the absolute values of E_{form} are converged with respect to cut-off energy and $\mathbf{k}$-point sampling to better than 0.1 eV. However, for the *relative* stability of structures with the same composition but different geometries and/or magnetic structures, we can give a much stricter error estimate, only several meV, due to error cancellation since all numbers entering the energy difference are calculated with the same technical settings. The degree of spin polarization at the Fermi level is quantified from the spin-resolved density of states (DOS), which is calculated using a finer $\mathbf{k}$-point mesh of $16 \times 16 \times 1$ in conjunction with the tetrahedron method for Brillouin integration. We note that a more realistic assessment of spin injection at the interface would have to consider the match in Fermi velocities in the film and the substrate. For bulk magnets, a spin polarization in-

cluding a suitable weighting with the Fermi velocity can be defined[29,30]. However, in this work we retain the more wide-spread definition of the DOS.

III. RESULTS AND DISCUSSION

A. bulk phases of MSi

Before studying the MSi thin films on Si(001), we briefly discuss the bulk phases of the TM mono-silicides MSi (M=Mn, Fe, Co, Ni). For all metal atoms discussed here, the mono-silicides have the same bulk crystal structure, the B20 structure, whose symmetry is characterized by the $P2_13$ space group.[31] Since the lattice constant of the cubic unit cell is around 4.5 Å for all these compounds, they cannot be lattice-matched with Si(001). However, the metastable CsCl phase calculated within DFT-GGA lies only slightly above the ground-state $P2_13$ structure in total energy, for M=Mn, Fe, Co, and Ni by 0.25, 0.04, 0.42, and 0.24 eV per formula unit, respectively. Moreover, it follows from our GGA calculations that the equilibrium lattice constants for the metastable CsCl phases are 2.79, 2.77, 2.78, and 2.85 Å, respectively. They are almost half the calculated lattice constant of Si (5.48 Å), and thus the lattice mismatch with Si(001) is less than 2% for the CsCl-like MnSi, FeSi, and CoSi, and 4% for NiSi. These results for MSi (M=Fe, Co) agree well with the previous calculations by Moroni, Podloucky, and Hafner.[8]

We show in Fig. 2 the density of states of the CsCl-like MSi calculated within GGA in the nonmagnetic (NM) state. The CsCl-like FeSi and NiSi have a low DOS at the Fermi level, which explains, within the framework of the Stoner model of magnetism, why we find them to be non-magnetic. In contrast, the Fermi level of the CsCl-like MnSi lies at a falling shoulder of the t_{2g} DOS. In particular, the Fermi level of the CsCl-like CoSi lies at a steep slope of the e_g DOS, which gives rise to Stoner FM instability. This has also been discussed by Profeta et al.[11] Our calculations show that the FM ground state of CoSi has a spin moment of 0.63 μ_B/Co and a lower total energy than the NM state by 16 meV per formula unit.

Since epitaxial growth of the CsCl-like FeSi and CoSi films on Si(111) has already been achieved by von Känel et al.,[9,10] and given that CoSi has the highest energy difference for the metastable phase among the CsCl-like MSi (M=Mn,Fe,Co,Ni), we consider it likely that growth of the CsCl-like MSi films on Si(001), and of the CsCl-like MnSi and NiSi films on Si(111), can be achieved as well.

B. MSi thin films on Si(001)

For various amounts of TM atoms deposited on Si(001), we perform calculations to investigate the sta-
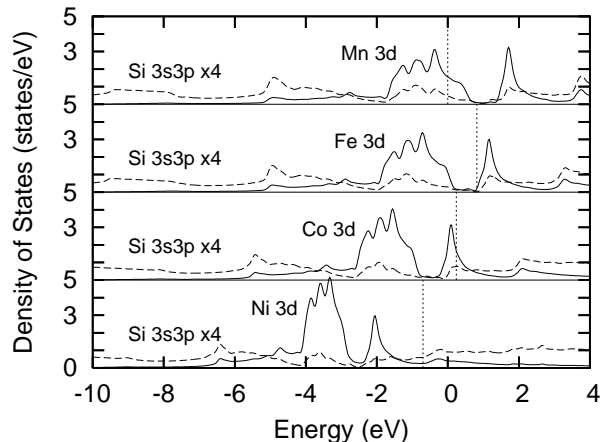

FIG. 2: Orbital-projected DOS of metastable CsCl-like bulk MSi (M=Mn, Fe, Co, Ni) in the non-magnetic state. The solid lines refer to the M 3d bands, which split into the lower-lying t_{2g} and the higher-lying e_g bands. The dashed lines refer to the Si 3s3p states (magnified four times for clarity). The Fermi level of MnSi (calculated to be 11.76 eV) is used as energy zero for all plots. The Fermi levels (vertical dotted lines) of FeSi, CoSi, and NiSi differ from that of MnSi by 0.81, 0.23, and −0.69 eV, respectively. Obviously, the shapes of those DOS are similar, and the Fermi level shifts towards and strides over the e_g states to accommodate more and more d-electrons as M varies from Mn through Fe and Co to Ni. Note that, as M varies from Mn to Ni, the M 3d bands monotonously shift down toward the Si 3s3p valence bands.

ble binding sites or the (meta-)stable atomic structure of films. As seen below, the preceding calculations for θ=0.5 ML and 1 ML are helpful to understand why the M atoms prefer subsurface sites and the Si atoms sit in the topmost layer.

We start our calculations by considering a coverage of θ =0.5 ML of metal atoms M, occupying either atomic sites on the surface [cf. Fig. 1(a)] or subsurface sites [cf. Fig. 1(b)] of Si(001). The results show that all metal adsorbates, M=Mn, Fe, Co, and Ni, are generally more stable at Si(001) subsurface than at surface sites, by about 0.1 eV per (1×1) cell for M=Mn, and more than 0.4 eV for M=Fe, Co, or Ni, as seen in Table I. The surface adatoms M=Mn, Fe, and Co have a sizable spin moment, and in Table II, the values within the atomic muffin-tin spheres are reported. The reduction of the spin magnetic moment of M atoms on subsurface sites is due to the increased number of M-Si bonds. In particular, the magnetic moment of the subsurface Co atom is almost completely quenched. Moreover, we find Ni atoms to have vanishing magnetic moments both on the surface and at subsurface sites. Note that in these M-Si (M=Mn, Fe, Co) systems, spin moments are also induced on the Si atoms adjacent to M, albeit smaller than 0.1 μ_B.

Secondly, we compare two possible atomic structures for 1 ML coverage, the 1ML-M surface mixed layer [cf.

TABLE I: Formation energies [in units of eV per (1×1) cell] of films in various structures depicted in Fig. 1, labelled a)–f), relative to the clean Si(001) surface and elemental bulk M=Mn, Fe, Co, or Ni. Note that the values of E_{form} in the M=Mn row are slightly different (by 0.03 eV at most) from those of our previous calculations[5] given in parenthesis, due to different values of the muffin-tin radius of Si and the cut-off energy used.

E_{form}	a	b	c	d	e	f
Mn	0.76	0.67	0.89	0.61	−0.43	−1.55
	(0.77)	(0.68)	(0.90)	(0.62)	(−0.40)	(−1.53)
Fe	1.11	0.67	0.93	0.01	−1.71	−3.78
Co	0.99	0.47	0.89	−0.44	−2.38	−4.15
Ni	0.59	0.18	0.22	−0.64	−2.37	−3.46

Fig. 1(c)] and the layered Si-M film [cf. Fig. 1(d)]. Our results show that the latter is energetically more favorable than the former, by about 0.3 eV per (1×1) cell for M=Mn and around 1.0 eV for M=Fe, Co, or Ni. Next, we analyse the chemical bonding in these systems. We start by noting that M (=Mn, Fe, Co, or Ni) and Si have almost identical electronegativity of 1.6 or 1.7, and hence form strong covalent bonds. From Fig. 3, we see that the M-Si bonds have similar covalent charge density as the Si-Si bonds. Moreover, for all relaxed structures of the Si-M/Si(001) (M=Mn, Fe, Co) films, we find that both the substitutional M (named $M1$) and the interstitial M (named $M2$) each have four M-Si bonds which are shorter, by 0.13 Å at least, than the sum of the M and Si atomic radii, due to covalent bond contraction. NiSi is an exception to this general trend; in Si-Ni/Si(001) the substitutional Ni1 has four shrunk Ni-Si bonds which are contracted by 0.08 Å, and the interstitial Ni2 has only two short Ni-Si bonds, contracted by 0.18 Å. This exceptional behavior, both the smaller Ni1-Si bond-shortening and the reduced number of short Ni2-Si bonds, can be understood by considering that the number of empty $3d$ orbitals available for bonding with Si decreases in the TM series from Mn to Ni. Note that the transition metal atoms are seven-fold coordinated to Si in the natural bulk silicides MSi, and eight-fold coordinated in MSi$_2$. Thus,

TABLE II: Spin magnetic moment (in unit of μ_B) of M atoms within muffin-tin spheres for various structures depicted in Fig. 1, labelled a)–d). NM Ni case is omitted. Reported for c) are both values for the surface and subsurface M atoms, separated by a comma; and for d) are the substitutional and interstitial M atoms.

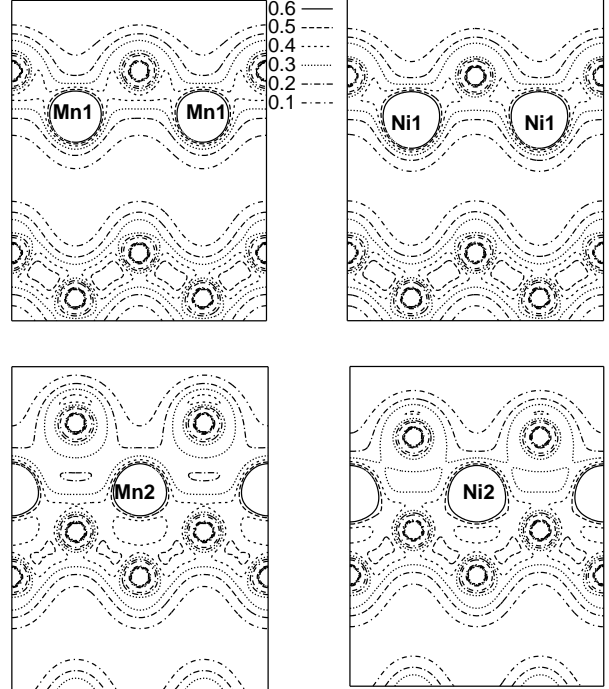| m	a	b	c	d
Mn	3.68	3.08	3.26, 2.25	2.16, 1.65
Fe	2.35	2.09	2.45, 1.94	0.11, 0.05
Co	0.95	0.03	0.45, −0.07	0.41, 0.35

FIG. 3: Valence charge density in the $(1\bar{1}0)$ plane for 1 ML Si-capped silicide films, Si-M/Si(001) [M=Mn (left panels) or Ni (right panels), cf. Fig. 1(d)]. The cuts are chosen to contain the substitutional-$M1$ and Si (upper row), or the interstitial-$M2$ and Si atoms (lower row). Contour lines from 0.1 to 0.6 e/Å^3 in steps of 0.1 e/Å^3 are shown. The Mn-Si and Ni-Si bonds have a covalent charge density as high as 0.4 e/Å^3, similar to the Si-Si bonds with 0.5 e/Å^3.

the subsurface TM layer capped by a Si layer in the Si-M/Si(001) films optimizes the surface covalent bonding structure, since it allows for the optimum fourfold coordination of the capping Si atoms, while simultaneously increasing the coordination of the M atoms (compared to *on surface* adsorption). The Si-termination of the CsCl-like FeSi/Si(111) film surface has been previously verified both experimentally and theoretically.[32] Moreover, the Si capping layer, due to the doubled atomic density as compared with the Si(001) substrate, displays strong buckling, 0.43, 0.57, 0.47, and 0.21 Å in the Si-M/Si(001) film with M=Mn, Fe, Co, or Ni, respectively.

Since the layered Si-M film has turned out to energetically most favorable from the above calculations, we employ the same atomic structure to multilayered Si-M [n(Si-Mn)] films, i.e., to the CsCl-like MSi films with Si termination, as depicted in Figs. 1(e) and 1(f). As seen in columns (d), (e) and (f) of Table I, The formation energy E_{form}, defineded according to Eq. (1), decreases monotonously with increasing film thickness for all CsCl-like MSi films. This decrease is a consequence of the heat of formation released for each formula unit of MSi formed from the elements. The onset of negative E_{form} at $\theta \approx 2$ ML Mn or 1 ML M (M=Fe, Co, Ni)

indicates that the films are stable against decomposition into the clean Si(001) surface and elemental bulk M.

Moreover, the thermodynamic stability of the MSi films increases as M varies from Mn through Fe, Co to Ni at $\theta < 2$ ML. We attribute this finding to the increasing M–Si bond strength: Note that E_{form} is calculated with reference to the clean Si(001) surface and elemental TM bulk (see Eq. 1). Both GGA calculations and experimental measurements agree that the cohesive energies of Fe, Co, and Ni are very similar, and higher than that of Mn by about 1 eV.[26] Therefore the decreasing E_{form} of the MSi films at $\theta < 2$ ML as M varies from Mn to the later TMs indicates that the binding energy of the M atoms on Si(001) increases more strongly so as to overcompensate the rise in the removal energy of an M atom from its bulk reservoir upon variation of M from Mn to the later TMs. Hence, the strength of the M–Si bonds must increase accordingly. This trend can be understood by observing that the M $3d$ bands increasingly come into resonance with the Si $3s3p$ valence bands due to decreasing energy separation between them (see Fig. 2), because the M $3d$ level shifts down towards the Si $3s3p$ level as the atomic number of the transition metal increases. However, the trend is reversed for the NiSi film at $\theta = 2$ ML [see column (e) in Table I]. For thicker MSi films, the order of thermodynamic stability, quoted from low to high, changes to M=Mn, Ni, Fe, Co at $\theta = 3$ ML [see column (f) in Table I]. The anomaly in the NiSi case can be explained in terms of M $3d$ orbital occupation. Since Ni has the fewest empty $3d$ orbitals available for bonding with Si, the Ni atoms in the NiSi film (except for the interfacial Ni) being eightfold coordinated to Si become oversaturated. The oversaturation for eightfold Si coordination of Ni is also reflected by the increased lattice constant of the CsCl-like NiSi [compared with MSi (M=Mn,Fe,Co) as seen in Sec. III. A]. This interpretation is corroborated by the experimental observation that the lattice constant of the eightfold coordinated NiSi$_2$ is larger than that of CoSi$_2$.

The above results are helpful to understand three experimental observations. Firstly, pre-adsorbed Co has been found to improve the quality of Fe films grown on Si(001).[33] Our calculations show that Co–Si bonds are stronger than Fe–Si bonds; hence the improved film quality can be explained by a CoSi layer forming at the interface which prevents interdiffusion between the Fe overlayer and the Si substrate. Moreover, we can predict that Ni cannot be used for this purpose, because the highly Si-coordinated Ni-silicide is thermodynamically less stable than Fe-silicide, as we reported above. Hence, we conclude from our calculations that Ni is unsuitable for a barrier layer to suppress the intermixing between Fe and Si. Secondly, the trends in bond strength revealed by our calculations help to explain the structure of Heusler alloys with the chemical composition M_2MnSi (M=Fe,Co,Ni), or more generally X_2YZ,[2,3,4] in which X, Y and Z have a similar electronegativity and Y possesses a robust magnetic moment. In these

materials, so-called full Heusler alloys, which can be considered as a (111) stacking of layers with the sequence $Z - X - Y - X - Z - X - Y - X - Z \ldots$, it is always the element X capable of making stronger bonds to Z which occurs in the layers adjacent to Z, while the more weakly bonding element Y has Z only as its second neighbors. Together with knowledge of the energetic positions of the atomic levels of the X, Y, and Z atoms, and thus of their relative bond strengths, this rule can be used as heuristics in the search for new Heusler alloys (some of which may be half-metallic FMs), somewhat similar in spirit to the 'band gap engineering' done in semiconductor physics. Thirdly, on the basis of our results, we can explain the observed site selectivity[34] for substitution of other TMs in the Heusler alloy Fe$_2^A$Fe^{B}Si: The TMs to the right of Fe in the periodic table, Co and Ni, making stronger bonds to Si than Fe itself, substitute for Fe^A to form new stronger bonds with four Si neighbors. The earlier TMs Ti, V, Cr, Mn, however, substitute for Fe^B, thus preserving the stronger Fe^A-Si bonds.

Next we turn to the magnetism of the MSi thin films on Si(001) [n(Si-M)/Si(001)]. As a general trend in the pseudomorphic (Si-M)/Si(001) films [cf. Fig. 1(d)], we find that the substitutional $M1$ (cf. Fig. 3) has a little larger spin moment (e.g., 2.16 μ_B/Mn1) than the interstitial $M2$ (e.g., 1.65 μ_B/Mn2), as seen in Table II. This can be partly ascribed to the number of M-Si bond being fewer by one for $M1$ (six-fold coordination) than $M2$ (seven-fold coordination). First, we describe in more detail the results for MnSi films. The (Si-Mn)/Si(001) film is found from our calculations to be a ferromagnetic metal with a sizable spin moment, in which the Si atoms mediate the FM Mn-Mn coupling via hybridization between the Si $3s3p$ and Mn $3d$ itinerant electrons. A vital role is played by the capping Si atoms; in their absence the bare Mn film on Si(001) is found to be antiferromagnetic (AFM).[5] For the 2(Si-Mn)/Si(001) film, our calculations also predict a FM metallic ground state. The 3(Si-Mn)/Si(001) film is found to be ferrimagnetic with FM (ferrimagnetic) intra (inter)-layer coupling, as seen in Tables III and IV. The middle Mn layer has a small spin moment of $-0.14\,\mu_B$/Mn antiparallel to the larger one of 1.74 μ_B/Mn in the interfacial Mn layer. It mediates a superexchange ferrimagnetic coupling between the interfacial and subsurface Mn layers. Note that the interlayer magnetic coupling is weak in the n(Si-Mn)/Si(001) thin films, e.g., the energy cost for flipping the magnetic moments of one layer, i.e., going from FM to AFM ordering between layers, is 8 and 10 meV/Mn in the 2(Si-Mn)/Si(001) and 3(Si-Mn)/Si(001) films, respectively. However, the FM intralayer coupling is rather strong, as is evident from the energy cost for flipping one of the two magnetic moments per layer in the unit cell, i.e., going from FM to AFM ordering within the layers, which we calculate to be 70–80 meV/Mn. Moreover, the various magnetic MnSi films we studied have a spin polarization of carriers at the Fermi level in the range of 30–50%.[5] These results imply that the ultrathin MnSi

TABLE III: Spin magnetic moment (in unit of μ_B) of atoms averaged over one layer [from interface layer (left) to surface layer (right)] of the MSi thin films on Si(001) [cf. Figs. 1(d), 1(e) and 1(f)] in their respective magnetic ground states. Note that the FeSi/Si(001) films are non-magnetic, as discussed in the text. The non-magnetic NiSi/Si(001) films are omitted.

	M	Si	M	Si	M	Si
Si-Mn	1.90	−0.05				
Si-Fe	0.08	−0.01				
Si-Co	0.38	0.02				
2(Si-Mn)	1.90	−0.07	1.11	0.02		
2(Si-Fe)	0.38	−0.01	0.06	0.01		
2(Si-Co)	0.16	−0.01	0.55	−0		
3(Si-Mn)	1.74	−0.03	−0.14	0.03	−1.07	−0.04
3(Si-Fe)	0.31	−0.01	0.01	−0	0.01	+0
3(Si-Co)	0.38	−0.01	0.56	−0.01	0.63	−0.01

TABLE IV: Total-energy difference (in units of meV per M atom) of the n(Si-M)/Si(001) (n=1,2,3; M=Mn,Fe,Co) thin films among the ferromagnetic (FM), antiferromagnetic [AFM, either intra- (or inter-) layered AFM marked with superscript i (or o)], and non-magnetic (NM) states.

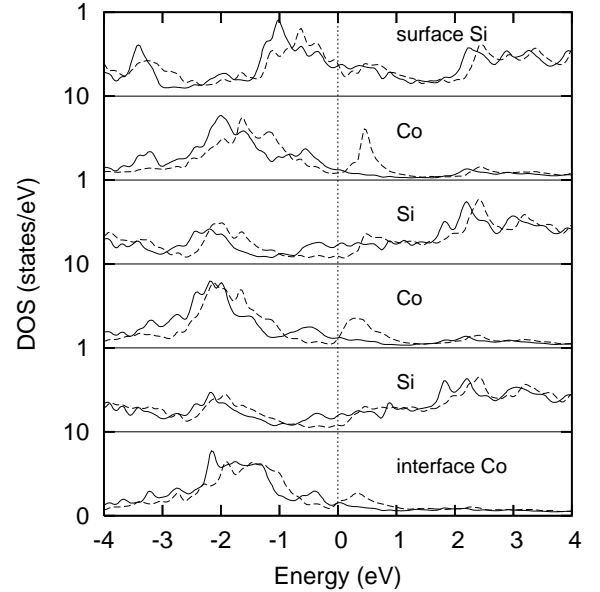|	n(Si-Mn)			n(Si-Fe)			n(Si-Co)		
n	1	2	3	1	2	3	1	2	3
FM	0	0	10	0	0	0	0	0	0
AFM	71^i	8°	0°	FM	0	0	NM	0	10°
NM	350	188	80	0	5	0	15	17	28

FIG. 4: The layer-resolved DOS of the FM 3(Si-Co)/Si(001) film. The layers are shown from surface (top) to interface (bottom) for the atomic structure depicted in Fig. 1 (f). Full lines show the majority spin, dashed lines the minority spin component.

film on Si(001) is a candidate for magnetoelectronic materials.

For the (Si-Fe)/Si(001) film, our calculations find the AFM state to be unstable and to converge to the FM ground state (with a very small spin moment, as seen in Tables III and IV). However, the FM state and the NM state are energetically degenerate, as seen in Table IV. Similarly, the FM state of the 2(Si-Fe)/Si(001) and 3(Si-Fe)/Si(001) films has a small spin moment and almost the same energy as the NM state, the energy difference being less than 5 meV/Fe. Therefore we conclude that the FeSi/Si(001) films are NM, like the CsCl-like FeSi bulk, as discussed in Sec. III.A. The NiSi/Si(001) film is also NM, as evidenced by our computational results that both FM and AFM states converge to the NM ground state.

In strong contrast to the NM FeSi and NiSi films on Si(001), the CoSi films on Si(001) have a FM ground state. This is evident from the magnetic moments reported in Table III and from the energetics reported in Table IV. In our calculations, a hypothetical AFM state of (Si-Co)/Si(001) converges to a NM state which is, however, higher in total energy than the FM ground state by

15 meV/Co. The 3(Si-Co)/Si(001) film is also FM with a sizable spin moment in the middle layer (well comparable with the bulk value of 0.63 μ_B/Co), unlike the ferrimagnetic 3(Si-Mn)/Si(001) film. For 3(Si-Co)/Si(001), the layered AFM state is higher in total energy than the FM ground state by 10 meV/Co. Moreover, our calculations find an increasing energy difference between the FM ground state and the NM state: 15, 17 and 28 meV/Co in the (Si-Co), 2(Si-Co) and 3(Si-Co)/Si(001) films, respectively. We show in Fig. 4 the layer-resolved DOS of the FM 3(Si-Co) overlayers. The Fermi level is found to be close to a minimum of the Co 3d DOS. Obviously the high DOS at the Fermi level seen in Fig. 2 for hypothetical NM CoSi has transformed into a minimum of the FM DOS due to exchange splitting. For this reason, the FM state is stable. Analyzing the DOS projected onto each Si overlayer, we find a considerable spin polarization of carriers at the Fermi level in the interior and near-interface Si overlayers, although those Si atoms themselves possess only a tiny induced spin moment.

These results suggest that the CsCl-like CoSi/Si(001) films are interesting materials systems, having a high thermodynamic stability among the MSi/Si(001) films (see Table I) and a FM metallic ground state. Since the epitaxial growth of the CsCl-like CoSi film on Si(111) has already been achieved,[10] attempting to grow a CoSi/Si(001) film may be worth the experimental effort. Moreover, the predicted ferromagnetism of the CsCl-like CoSi calls for experimental investigations.[35]

C. M_2MnSi thin films on Si(001)

In this Section, we study films of the Heusler alloys M_2MnSi (M=Fe, Co, Ni), which one can think of as being formed by partial Mn substitution for Si in the CsCl-like MSi films (cf. Fig. 1) described so far. In particular, the Heusler alloy Co$_2$MnSi is of interest here, since its bulk FM half-metallicity predicted by band calculations attracts much attention both from the experimental[36,37,38] and theoretical[2,3,4,39,40] side. Bulk Fe$_2$MnSi, in an ideal FM state, is also predicted by band calculations to be half-metallic.[41] However, calculations allowing for non-collinear alignment of the magnetic moments have found that, in the ground state, the Mn magnetic moments are canted with respect to the direction of the Fe magnetic moments,[42] which leads to partial compensation of the magnetic moments along the [111] axis. The hypothetical compound Ni$_2$MnSi, which has not been synthesized so far to our knowledge, is shown by our calculations *not* to be half metallic. For the Co$_2$MnSi(001) surface, it has been shown recently by means of DFT calculations[21] that the termination by a Mn-Si crystal plane is thermodynamically stable, but a purely Mn- or purely Si-terminated surface can be stable as well under very Mn-rich or under very Si-rich conditions, respectively.

The goal of this work is to investigate how finite-size effects and epitaxial strain in very thin films affect the magnetic properties. The latter effect, lowering the crystallographic symmetry, could possibly change the half-metallicity of Co$_2$MnSi and Fe$_2$MnSi films. In particular, we investigate how possible surface and interface electronic states affect the electronic and magnetic properties of the films. To this end, we perform systematic studies as a function of film thickness. Moreover, we consider various possibilities for the surface termination of the films, either Si surface termination [cf. Figs. 5(a) and 5(b)] or MnSi termination [cf. Figs. 5(c), 5(d), and 5(e)]. Note that the M=Fe, Co, or Ni termination is energetically unfavorable for reasons discussed in the previous Section, and thus disregarded in this work. In addition to the two types of surface termination, two types of interfaces are studied, namely the M/Si interface (cf. Fig. 5) and the MnSi/Si interface. The latter is characterized by extra Mn atoms occupying the interstitial sites of the interfacial Si layer (not shown). Firstly, we study the M_2MnSi/Si(001) films with Si termination and M/Si interface. Secondly, we deal with films with MnSi termination and M/Si interface. Thirdly, we discuss also the MnSi/Si interface, but restrict ourselves to Co$_2$MnSi/Si(001) films, since they are thermodynamically stable and have a robust FM metallic ground state, as seen below, and hence are most relevant.
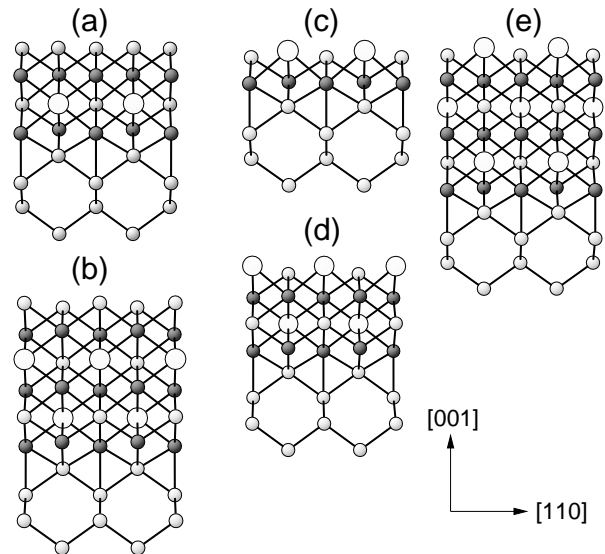

FIG. 5: Side view of the Si-terminated two-layered (a) and three-layered (b) Heusler alloy M_2MnSi (M=Fe, Co, Ni) films on Si(001) with M/Si interface, and of the MnSi-terminated one-layered (c), two-layered (d), and three-layered (e) M_2MnSi films. Black balls represent M, gray balls Si, and large white balls Mn atoms. The bonds shorter than 2.65 Å are shown.

1. M_2MnSi/Si(001): Si termination and M/Si interface

In this Section, we use the terms two-layered [cf. Fig. 5(a)] and three-layered [cf. Fig. 5(b)] Heusler alloy films, according to the film thickness measured in repetition periods of the atomic superstructure of the alloy. Firstly, we discuss the results for the two- and three-layered films, focussing on magnetic ordering. Independent on composition, we find for all the two-layered M_2MnSi films a metallic ground state with FM coupling both in the Mn sublattice and between the Mn- and M-sublattices (M=Fe,Co,Ni). For Fe$_2$MnSi, AFM ordering among the magnetic moments of Fe and Mn is metastable, but higher than the FM state in total energy by 20 meV per (1×1) cell. For the Co$_2$MnSi and Ni$_2$MnSi films, however, AFM ordering of the magnetic moments of the Co and Mn (or of Ni and Mn, respectively) is found to be unstable, and the calculations converge to the FM ground state. Moreover, our results show that the effective Mn-Mn FM coupling is strong, since the calculated energy cost to flip a Mn-Mn spin pair from parallel to anti-parallel orientation is as high as 73 meV/Mn in Fe$_2$MnSi, 216 meV/Mn in Co$_2$MnSi, and 80 meV/Mn in Ni$_2$MnSi. Note that in the two-layered M_2MnSi films, the Mn atoms have the same environment as in the bulk. Therefore it is not surprising that the calculated Mn-Mn coupling strengths approximately scale with the measured FM Curie temperatures of 219 K for Fe$_2$MnSi, 985 K for Co$_2$MnSi, and 320, 344, and 380 K for Ni$_2$MnZ (Z=Sn,Ge,Ga, respectively).[2,3]

Secondly, we analyze the spin magnetic moments in the films (see Table V). On the one hand, the Mn spin moment, being generally larger than 2 μ_B, increases in the M_2MnSi films as M varies from Fe through Co to Ni, following the same trend as in the bulk materials. This finding can be at least partly ascribed to decreasing d-d hybridization among Mn and the neighboring transition metal atoms when going from Fe to Ni, in accordance with the increasing energy separation between the Mn 3d and M 3d orbitals (see Fig. 2). On the other hand, one can argue that the Mn spin moment in the M_2MnSi/Si(001) films is still smaller than that in the M_2MnSi bulk. Again, this can be explained by stronger in-plane d-d hybridization in the film compared to the bulk, which gives rise to more delocalized planar electronic states and a reduced magnetic moment. The reason for this anisotropy is that the lattice constant of bulk Si is about 4% smaller than that of cubic M_2MnSi. Hence the M_2MnSi films have reduced planar lattice constant under the epitaxial constraint. The transition metal atom M(=Fe,Co,Ni) has a spin moment less than 1 μ_B. In addition, the Si atom in the MnSi layer has a small induced spin moment which is opposite to the spin moment of the neighboring metal atom, and generally smaller than 0.05 μ_B/Si. The substrate Si atoms have an even smaller spin moment of less than 0.02 μ_B/Si oscillating in its orientation between one substrate layer and the next one.

For the Si-terminated three-layered M_2MnSi films, our calculations find, in complete analogy to the above two-layer case, a FM metallic ground state irrespective of the nature of the transition metal. Besides the strong FM Mn-Mn intralayer coupling discussed above, the interlayer Mn-Mn coupling (evaluated by switching the relative orientation of the magnetic moment in two neighboring MnSi layers in the supercell) is 4 meV/Mn in the Fe$_2$MnSi film, 167 meV/Mn in Co$_2$MnSi, and 30 meV/Mn in Ni$_2$MnSi. The reduced interlayer coupling can be at least partly ascribed to a tetragonal distortion, by noting that the Heusler alloy film is under compressive epitaxial strain on Si(001), as stated above, and thus has an enlarged spacing between layers. In addition, the M spin, which mediates the effective Mn-Mn coupling, plays an important role for the magnetic ordering. Note that in the three-layered M_2MnSi films, the M atoms in the layer sandwiched between two MnSi layers have an averaged spin moment of 0.21 μ_B/Fe, 0.95 μ_B/Co, and 0.28 μ_B/Ni, as seen from Table V. In contrast to this, we observe that for the layered AFM ordering of the Mn spins, the Co spin in the middle layer is quenched to a value close to zero. The vanishing of the Co spin moment in the layered AFM state, sitting between two spin-antiparallel MnSi layers, is simply a consequence of symmetry. The highest energy cost of switching from FM to AFM alignment of the Mn spins correlates with the largest magnetic moment at Co in the FM state in the three Heusler alloys studied here. This indicates that the quenching of the Co spin moment is energetically unfavourable and hence the
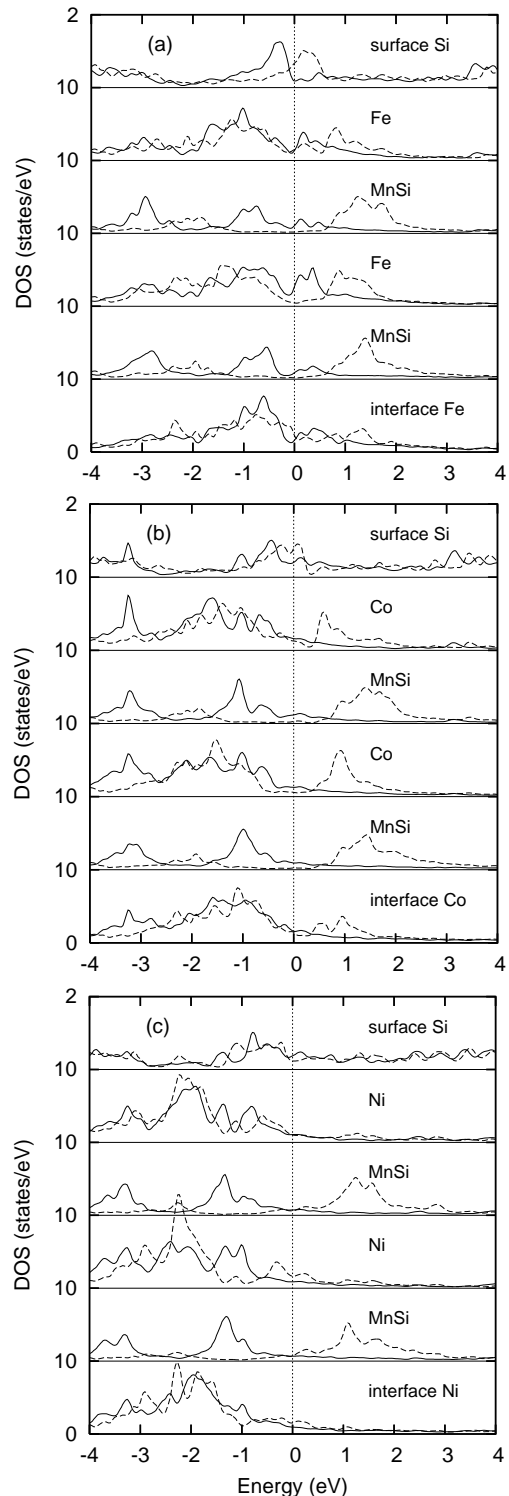

FIG. 6: The layer-resolved DOS of the Si-terminated three-layered Fe$_2$MnSi (a), Co$_2$MnSi (b) and Ni$_2$MnSi (c) films on Si(001) with M/Si (M=Fe, Co, or Ni) interface. In each panel, the overlayers are shown from surface (top) to interface (bottom) for the atomic structure depicted in Fig. 5(b). Full lines show the majority spin, dashed lines the minority spin component.

TABLE V: The layer-resolved (counted from the substrate to the surface) atomic spin moments (in unit of μ_B) of the Si-terminated two-layered (2L) and 3L M_2MnSi/Si(001) films and of the MnSi-terminated 1L, 2L and 3L M_2MnSi/Si(001) films (cf. Fig. 5). All films have a M/Si interface. Shown in the last three rows are the calculated atomic spin moments of Fe$_2$MnSi and Co$_2$MnSi at the experimental lattice constant and of Ni$_2$MnSi (not yet synthesized) at the GGA optimized lattice constant.

Si-term.	M	Si4	Si3	Si2	Si1	M	MnSi	M	MnSi	M	Si
	Fe	0.003	−0.001	0.015	−0.007			0.61	2.24/−0.02	0.36	0.14
2L	Co	0.005	0.005	0.013	−0.005			0.55	2.77/−0.04	0.70	0.01
	Ni	−0.002	−0.006	−0.002	−0.009			0.14	3.06/−0.04	0.13	−0.02
	Fe	0.001	−0	0.011	−0	0.20	2.20/−0.01	0.21	2.31/−0.01	0.35	0.08
3L	Co	0.004	0.005	0.007	−0.006	0.53	2.74/−0.04	0.95	2.72/−0.04	0.71	−0.01
	Ni	0	−0.003	0.004	−0.007	0.16	3.03/−0.03	0.28	3.14/−0.04	0.12	−0.02

MnSi-term.	M	Si4	Si3	Si2	Si1	M	MnSi	M	MnSi	M	MnSi
	Fe	0.001	0	0.010	−0.005					0.84	3.42/−0.10
1L	Co	0	0.002	0.005	−0					0.42	3.56/−0.10
	Ni	−0.001	−0.002	0.001	−0.007					0.02	3.58/−0.10
	Fe	0.002	−0.002	0.018	−0.010			0.64	2.09/−0.02	−0.06	3.45/−0.10
2L	Co	0.005	0.004	0.013	−0.011			0.54	2.65/−0.05	0.82	3.52/−0.12
	Ni	−0.001	−0.004	−0.001	−0.005			0.18	3.05/−0.03	0.23	3.63/−0.10
	Fe	0.001	−0.002	0.011	−0.007	0.47	2.21/−0.02	0.01	2.17/−0	0.18	3.50/−0.11
3L	Co	0.004	0.003	0.008	−0.013	0.52	2.70/−0.04	0.99	2.73/−0.04	0.86	3.53/−0.11
	Ni	0	−0.003	0.002	−0.006	0.15	3.06/−0.03	0.29	3.12/−0.04	0.17	3.61/−0.11

bulk M_2MnSi	M	Mn	Si
Fe$_2$MnSi	0.083	2.769	−0
Co$_2$MnSi	0.987	3.013	−0.039
Ni$_2$MnSi	0.290	3.330	−0.028

FM state is preferred over the AFM state.

Next, we investigate if the half-metallic properties of the Co$_2$MnSi and Fe$_2$MnSi bulk materials also show up in the thin films. In Fig. 6, the overlayer-resolved DOS of the Si-terminated three-layered M_2MnSi (M=Fe,Co,Ni) films on Si(001) is shown. Generally, the films do not show a gap in the DOS at the Fermi level. However, the spin-polarization at the Fermi level is high in the three middle layers, MnSi-Fe-MnSi or MnSi-Co-MnSi. We interpret this as an incipient recovery of the half-metallicity of the bulk Fe$_2$MnSi and Co$_2$MnSi. However, in the Ni$_2$MnSi film, this is not the case, consistent with our finding that bulk Ni$_2$MnSi is *not* half-metallic. In all the M_2MnSi films studied here, the surface Si layer has a sizable spin-polarization (>30%) at the Fermi level, following the definition in Ref. 5, while the subsurface M and the interfacial M layers have only low spin-polarization (<10%) at the Fermi level (except for ∼20% for the interfacial Ni layer).

Finally, we turn to the subject of thermodynamic stability. By calculating the formation energy using Eq. (1), we conclude that all Si-terminated two- and three-layered M_2MnSi films on Si(001) are stable against a decomposition into the clean Si(001) surface and bulk TMs. This is indicated by their negative E_{form} values, as seen in Table VI. Moreover, we checked the stability of the M_2MnSi films against separated MSi and MnSi films by calculating the heat of reaction, ΔE, defined by

$$M\text{Si/Si(001)}+\text{MnSi/Si(001)}$$
$$\rightarrow M_2\text{MnSi/Si(001)}+\text{clean Si(001)}+\Delta\text{E} \qquad (2)$$

The M_2MnSi films is stable (unstable) if ΔE is positive (negative). As shown by our results summarized in Table VI, the two-layered Fe$_2$MnSi film [ΔE=0.02 eV per (1×1) cell] is close to becoming unstable, and the three-layered one [$\Delta E = -0.65$ eV per (1×1) cell] is obviously unstable. The two-layered Co$_2$MnSi film is stable while the three-layered one tends to be unstable. However, the Ni$_2$MnSi film is stable against a phase separation into the NiSi and MnSi films. This is because the NiSi film is less stable due to its oversaturated eight-fold Si coordination of Ni, while the Ni$_2$MnSi film is stable, involving only four-fold Si coordination of Ni.

2. M_2**MnSi/Si(001): MnSi termination and M/Si interface**

Next we deal with the M_2MnSi/Si(001) thin films with MnSi termination [cf. Figs. 5(c), 5(d) and 5(e)]. The surface Mn atom has an increased spin moment of about 3.5 μ_B, and the surface Si atom also has an increased
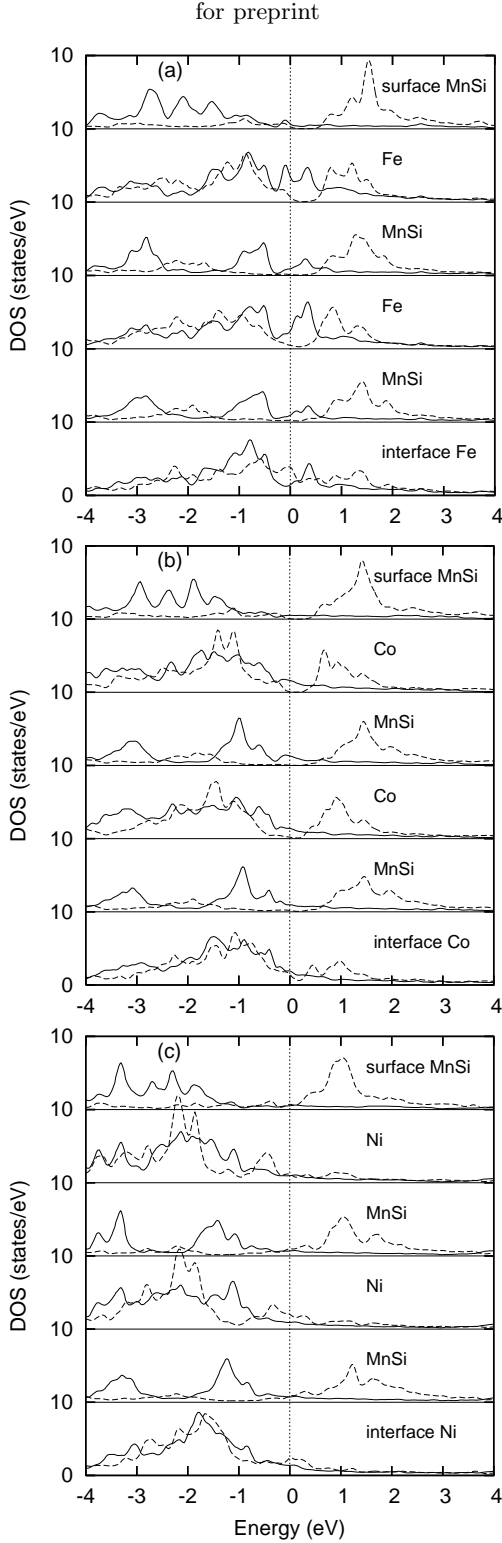
for preprint

FIG. 7: The layer-resolved DOS of the MnSi-terminated three-layered Fe$_2$MnSi (a), Co$_2$MnSi (b) and Ni$_2$MnSi (c) films on Si(001) with M/Si (M=Fe, Co, or Ni) interface. In each panel, the overlayers are shown from surface (top) to interface (bottom) for the atomic structure depicted in Fig. 5(e). Full lines show the majority spin, dashed lines the minority spin component.

TABLE VI: Formation energies (Eq. 1) and heat of reaction ΔE (Eq. 2) [in unit of eV per (1×1) cell] of the Si-terminated two-layered (2L) and 3L M_2MnSi/Si(001) films and of the MnSi-terminated 1L, 2L and 3L M_2MnSi/Si(001) films (cf. Fig. 5). All films have a M/Si interface.

	M	Si-term. $E_{\rm form}$	ΔE	MnSi-term. $E_{\rm form}$	ΔE
	Fe			−0.20	0.86
1L	Co			−0.71	0.92
	Ni			−0.80	0.81
	Fe	−1.08	0.02	−1.42	0.33
2L	Co	−1.87	0.14	−2.30	0.53
	Ni	−2.07	0.40	−2.37	0.62
	Fe	−2.51	−0.65	−2.87	−0.66
3L	Co	−3.48	−0.05	−3.99	0.09
	Ni	−3.42	0.58	−3.69	0.48

induced spin moment of about $-0.1\mu_B$, as seen in Table V. The spin moments of Mn and Si in the sandwich layer between two M layers are, due to the identical environment, very similar to those in the Si-terminated M_2MnSi films discussed above. The spin moment of the M atom sandwiching two MnSi layers, which plays an important role in the effective Mn-Mn coupling, is less than 0.2 μ_B/Fe, about 0.8-1.0 μ_B/Co or 0.2-0.3 μ_B/Ni. These values agree closely with those of the Si-terminated three-layered M_2MnSi films discussed above, and of the bulk materials. The MnSi termination brings about a gain in the formation energy in the range of 0.3-0.5 eV per (1×1) cell for the two- and three-layered M_2MnSi films (the exact value being materials-dependent) compared with the Si-terminated M_2MnSi films, which means that the former has higher thermodynamic stability. However, we would like to draw the reader's attention to the fact that the cohesive energy of Si is larger than that of Mn by about 1.5 eV, as indicated by experiments and our calculations. Combining the calculated values for the stability of both the films and the bulk phases, we conclude that the MnSi termination has highest thermodynamic stability mostly due to the low cohesive energy of Mn bulk. However, Si has a higher surface adsorption energy in the Si termination than Mn in the MnSi termination by about 1.0 eV. In this sense, the Si-terminated M_2MnSi films have stronger surface Si-M bonds than the Mn-M bonds present in the MnSi termination, and therefore the Si termination is chemically more stable. Moreover, as seen in Table VI, all the MnSi-terminated M_2MnSi films are stable against a phase separation, except for the three-layered Fe$_2$MnSi film.

In Fig. 7, the overlayer-resolved DOS of the MnSi-terminated three-layered M_2MnSi films are shown. The surface MnSi layer of the Fe$_2$MnSi film brings about a notable change for the subsurface Fe layer compared to the Si termination, as seen in Fig. 6(a), and this Fe layer
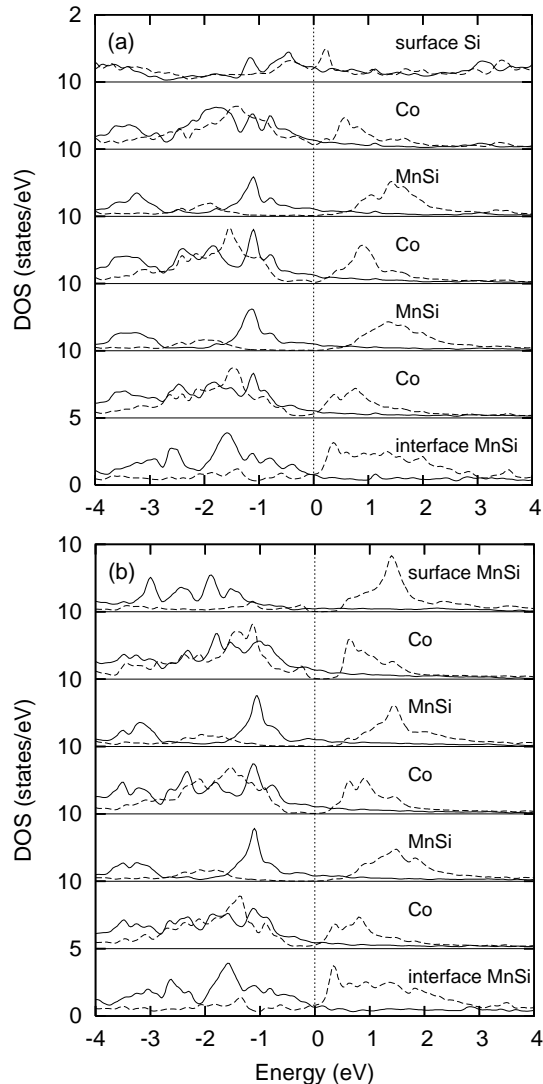
FIG. 8: The layer-resolved DOS of the Si-terminated (a) or MnSi-terminated (b) three-layered Co$_2$MnSi films on Si(001) with MnSi/Si interface. In each panel, the layers are shown from surface (top) to interface (bottom). Full lines show the majority spin, dashed lines the minority spin component.

now becomes highly spin-polarized ($\sim$65%) at the Fermi level. The three middle layers, MnSi-Fe-MnSi, are less affected. Again, we observe a tendency to recover the bulk half-metallicity. In addition, the interfacial Fe layer has a considerable spin-polarization ($\sim$45%) at the Fermi level. Similar changes occur in the MnSi-terminated Co$_2$MnSi films. In particular, the surface MnSi layer and the other overlayers, except for the interfacial layer, become almost half-metallic. However, for the Ni$_2$MnSi films, the surface MnSi layer brings no pronounced changes as compared with the Si termination.

3. Co$_2$MnSi/Si(001): MnSi/Si interface

When Mn atoms occupy the interstitial sites of the interfacial Si layer, as seen in Fig. 5, this layer now becomes a MnSi/Si interface, replacing the former Co/Si interface. Here we investigate Co$_2$MnSi/Si(001) films with this interface, considering two different surface terminations, either pure Si- or MnSi-termination. As seen in Table VII, the interfacial MnSi layer enhances the spin moments of the overlayers, especially of the near-interface Co layer, as compared with the Co$_2$MnSi/Si(001) film with the Co/Si interface (Table V). Comparing films with the same number of Co atoms, we find that the MnSi interface makes the films slightly more stable, through lowering the formation energy by 0.2 eV per (1$\times$1) cell or less for 1L, 2L, or 3L thickness (see Tables VI and VII for comparison), as a result of the low cohesive energy of bulk Mn which favors incorporation of extra Mn atoms. However, the Co/Si and MnSi/Si interfaces of the Co$_2$MnSi/Si(001) film differ by less than 0.2 eV, implying that chemical disorder in the interface layer could occur easily through thermal fluctuations. In addition, MnSi termination goes along with a gain in formation energy, compared with Si termination, about 0.5 eV per (1$\times$1) cell for the one-, two- and three-layered Co$_2$MnSi films with MnSi/Si interface, following the same trend as in the Co$_2$MnSi/Si(001) film with the Co/Si interface. In Fig. 8, the overlayer-resolved DOS of both the Si- and the MnSi-terminated three-layered Co$_2$MnSi/Si(001) films with MnSi/Si interface are shown. Although the interfacial Mn atom has almost the same spin moment as the middle MnSi layers where bulk half-metallicity is almost recovered, we observe that the spin polarization at the Fermi level in the interface layer is still tiny ($<$10%). Hence, in this respect, the MnSi/Si interface brings no pronounced change for the overlayers as compared to the Co$_2$MnSi/Si(001) film with Co/Si interface.

IV. CONCLUSION

In summary, we have presented systematic DFT-GGA calculations for pseudomorphic thin films of monosilicides MSi (M=Mn, Fe, Co, Ni) with CsCl-like atomic structure, and for thin films of Heusler alloys M_2MnSi (M=Fe, Co, Ni) on Si(001), with particular focus on the trends within the transition metal series.

Our calculations show that for pseudomorphic MSi films on Si(001), Si surface termination is energetically preferred because it optimizes the surface valence bond structure, i.e., four-fold coordination of surface Si and seven- or eight-fold coordination of subsurface M atoms are achieved. The M-Si chemical bond becomes stronger as M varies from Mn through Fe and Co to Ni, due to decreasing M 3d–Si 3s3p energy separation, and hence increasing hybridization of the metal 3d-states with the Si valence band. The calculated variations in thermodynamic stability of the MSi/Si(001) films can be ac-

TABLE VII: Formation energies [eV per (1×1) cell] either of the Si- or MnSi-terminated Co_2MnSi/Si(001) films with a MnSi/Si interface (cf. Fig. 5 but note that extra Mn atoms occupy the interstitial sites of the interfacial Si layer). The film thickness (1L, 2L, and 3L) refers to the number of the Co-MnSi bilayers. The third column shows the heat of reaction ΔE [eV per (1×1) cell], as defined in the text, Eq. 2. From the fourth column onwards, the overlayer-resolved (counted from the interface to the surface) atomic spin moments (in unit of μ_B) are shown. The substrate Si layers, each with an induced spin moment being generally less than 0.04 μ_B/Si, are omitted.

Si-term.	E_{form}	ΔE	MnSi	Co	MnSi	Co	MnSi	Co	Si
1L	−0.36	0.57					2.68/−0.02	0.78	0.01
2L	−1.98	0.21			2.87/−0.01	0.98	2.79/−0.04	0.74	0.02
3L	−3.54	−0.36	2.77/−0.01	1.04	2.82/−0.04	1.02	2.83/−0.04	0.81	0.03

MnSi-term.	E_{form}	ΔE	MnSi	Co	MnSi	Co	MnSi	Co	MnSi
1L	−0.92	1.09					2.74/−0.02	0.88	3.54/−0.10
2L	−2.48	0.35			2.80/−0.01	1.02	2.78/−0.05	0.87	3.53/−0.11
3L	−4.09	−0.49	2.78/−0.01	1.03	2.82/−0.04	1.06	2.78/−0.04	0.90	3.53/−0.11

counted for in terms of both the M $3d$–Si $3s3p$ energy separation and the M $3d$ orbital occupation.

These trends for the bond strength also enable us to rationalize the observed atomic ordering in Heusler alloys and to explain the experimentally observed site preference of transition metal impurities added to Heusler alloys. We confirm previous work[11] showing that CoSi films, in addition to ultrathin FM MnSi films[5], are another possibility to grow thin FM silicide films on Si(001), while FeSi and NiSi films are found to be non-magnetic. Therefore, MnSi and CoSi films on Si(001) deserve further experimental studies.

For the M_2MnSi/Si(001) films, our results show that MnSi termination is thermodynamically stable. The slightly less stable Si termination, once formed, is long-lived, since removing Si atoms is energetically more costly than removing Mn atoms. Except for the atoms in the surface and interface layers, we find that the electronic structure known from the bulk samples is recovered quickly in the interior of the overlayers. In particular, the half-metallicity of bulk Fe_2MnSi and Co_2MnSi is almost recovered in the three middle layers of the films investigated. As far as magnetic ordering in the M_2MnSi films is concerned, we find that the effective intralayer Mn-Mn FM couplings mediated by the first-neighbor M atoms are strong and approximately scale with the measured Curie temperatures of the corresponding bulk M_2MnSi samples. The interlayer Mn-Mn FM coupling remains strong in the Co_2MnSi films while it is (much) reduced in the Ni_2MnSi (Fe_2MnSi) films. The Co_2MnSi/Si(001) thin film is thermodynamically stable and has a robust FM metallic ground state, and thus is most relevant for possible applications. However, by analyzing our calculations we also identify two effects that could possibly be detrimental for use of these films for spin injection: The Co/Si and MnSi/Si interfaces are found to have a similar formation energy, which makes thermally induced interfacial disorder likely; and the interfacial Co or MnSi layer doesn't display the gap in the layer-resolved DOS of the minority spin channel characteristic for a half-metal.

[1] I. Žutić, J. Fabian, and S. D. Sarma, Rev. Mod. Phys. **76**, 323 (2004).

[2] J. Kübler, A. R. Williams, and C. B. Sommers, Phys. Rev. B **28**, 1745 (1983).

[3] S. Fujii, S. Ishida, and S. Asano, J. Phys. Soc. Jpn. **63**, 1881 (1994).

[4] I. Galanakis, P. H. Dederichs, and N. Papanikolaou, Phys. Rev. B. **66**, 174429 (2002).

[5] H. Wu, M. Hortamani, P. Kratzer, and M. Scheffler, Phys. Rev. Lett. **92**, 237202 (2004).

[6] N. Manyala, Y. Sidis, J. F. Ditusa, G. Aeppli, D. P. Young, and Z. Fisk, Nature Materials **3**, 255 (2004).

[7] M. K. Chattopadhyay, S. B. Roy, and S. Chaudhary, Phys. Rev. B. **65**, 132409 (2002).

[8] E. G. Moroni, R. Podloucky, and J. Hafner, Phys. Rev. Lett. **81**, 1969 (1998).

[9] H. von Känel, K. A. Mäder, E. Müller, N. Onda, and H. Sirringhaus, Phys. Rev. B **45**, R13807 (1992).

[10] H. von Känel, C. Schwarz, S. Goncalves-Conto, E. Müller, L. Miglio, F. Tavazza, and G. Malegori, Phys. Rev. Lett. **74**, 1163 (1995).

[11] G. Profeta, S. Picozzi, A. Continenza, and R. Podloucky, Phys. Rev. B **70**, 235338 (2004); G. Profeta, S. Picozzi, A. Continenza, G. Schneider, and R. Podloucky, J. Magn. Magn. Mater. **272-276**, e233 (2004).

[12] G. M. Dalpian, A. J. R. da Silva, and A. Fazzio, Surf.Sci. **566**–**568**, 688 (2004).

[13] A. P. Horsfield, S. D. Kenny, and H. Fujitani, Phys. Rev. B **64**, 245332 (2001).

[14] S. Higai and T. Ohno, Phys. Rev. B **62**, R7711 (2000).

[15] S. Kämmerer, S. Heitmann, D. Meyners, D. Sudfeld, A. Thomas, A. Hütten, and G. Reiss, J. Appl. Phys. **93**, 7945 (2003).

[16] S. Kämmerer, A. Thomas, A. Hütten, and G. Reiss, Appl. Phys. Lett. **85**, 79 (2004).

[17] J. Schmalhorst, S. Kämmerer, M. Sacher, G. Reiss, A. Hütten, and A. Scholl, Phys. Rev. B **70**, 024426 (2004).

[18] T. Ambrose, J. J. Krebs, and G. A. Prinz, J. Appl. Phys. **87**, 5463 (2000).

[19] W. H. Wang, M. Przybylski, W. Kuch, L. I. Chelaru, J. Wang, Y. F. Lu, J. Barthel, H. L. Meyerheim, and J. Kirschner, Phys. Rev. B **71**, 144416 (2005).

[20] I. Galanakis, J. Phys.: Condens. Matter **14**, 6329 (2002).

[21] S. J. Hashemifar, P. Kratzer, and M. Scheffler, Phys. Rev. Lett. **94**, 096402 (2005).

[22] S. Picozzi, A. Continenza, and A. J. Freeman, J. Phys. Chem. Solids **64**, 1697 (2003).

[23] S. Picozzi, A. Continenza, and A. J. Freeman, J. Appl. Phys. **94**, 4723 (2003).

[24] P. Blaha, K. Schwarz, G. K. H. Madsen, D. Kvasnicka, and J. Luitz, **WIEN2k***, an Augmented Plane Wave plus Local Orbitals Program for Calculating Crystal Properties*, K. Schwarz, Techn. Univ. Wien, Austria (2001), ISBN 3-9501031-1-2.

[25] J. P. Perdew, K. Burke, and M. Ernzerhof, Phys. Rev. Lett. **77**, 3865 (1996).

[26] P. H. T. Philipsen and E. J. Baerends, Phys. Rev. B **54**, 5326 (1996).

[27] E. G. Moroni, W. Wolf, J. Hafner, and R. Podloucky, Phys. Rev. B **59**, 12860 (1999).

[28] Using of the same RK_{max}=7.8 as in our previous work[5] but a little smaller $R_{Si}=R_{Fe}=R_{Co}=R_{Ni}$=1.06 Å (2.0 bohr) yields the higher cut-off energy of 15.2 Ryd, compared with that of 13.8 Ryd used previously. Consistence between our presently calculated results of the Mn/Si(001) system and those previously obtained, as seen in Table I, indicates that the technical settings used here ensure reliable numerical accuracy of our results.

[29] I. I. Mazin, Phys. Rev. Lett. **83**, 1427 (1999).

[30] R. P. Panguluri, G. Tsoi, B. Nadgorny, S. H. Chun, N. Samarth, and I. I. Mazin, Phys. Rev. B **68**, 201307(R) (2003).

[31] D. van der Marel, A. Damascelli, K. Schulte, and A. A. Menovsky, Physica B **224**, 138 (1998).

[32] S. Walter, R. Bandorf, W. Weiss, K. Heinz, U. Starke, M. Strass, M. Bockstedte, and O. Pankratov, Phys. Rev. B **67**, 085413 (2003).

[33] P. Bertoncini, P. Wetzel, D. Berling, G. Gewinner, C. UlhaqBouillet, and V. P. Bohnes, Phys. Rev. B **60**, 11123 (1999).

[34] T. J. Burch, J. I. Budnick, V. A. Niculescu, K. Raj, and T. Litrenta, Phys. Rev. B **24**, 3866 (1981).

[35] The FM ground state both of the CsCl-like CoSi bulk and the thin film on Si(001) is closely correlated with the crystal structure (eight-fold coordination) and the peculiar electronic band structure. Note that the natural CoSi at the B20 phase (seven-fold coordination) is found to be NM both in experiments and in our calculation. Moreover, our calculations show that for the CsCl-like CoSi thin film on Si(111), the 2(Si-Co)/Si(111) with seven-fold coordination is NM, while the 3(Si-Co)/Si(111) with eight-fold coordination is FM.

[36] M. P. Raphael, B. Ravel, M. A. Willard, S. F. Cheng, B. N. Das, R. M. Stroud, K. M. Bussmann, J. H. Claassen, and V. G. Harris Appl. Phys. Lett. **79**, 4396 (2001).

[37] L. Ritchie, G. Xiao, Y. Ji, T. Y. Chen, C. L. Chien, M. Zhang, J. Chen, Z. Liu, G. Wu, and X. X. Zhang, Phys. Rev. B **68**, 104430 (2003).

[38] L. J. Singh, Z. H. Barber, Y. Miyoshi, Y. Bugoslavski, W. R. Branford, and L. .F. Cohen Appl. Phys. Lett. **84**, 2367 (2004).

[39] S. Ishida, S. Fujii, S. Kashiwagi, and S. Asano, J. Phys. Soc. Jpn. **64**, 2152 (1995).

[40] S. Picozzi, A. Continenza, and A. J. Freeman, Phys. Rev. B **66**, 094421 (2002).

[41] S. Fujii, S. Ishida, and S. Asano, J. Phys. Soc. Jpn. **64**, 185 (1995).

[42] P. Mohn and E. Supanetz, Phil. Mag. B **78**, 629 (1998).